Cerebral Cortex, April 2016;26: 1634–1646

doi: 10.1093/cercor/bhu324
Advance Access Publication Date: 19 January 2015
Original Article

ORIGINAL ARTICLE

The Organization of Right Prefrontal Networks Reveals Common Mechanisms of Inhibitory Regulation Across Cognitive, Emotional, and Motor Processes

B. E. Depue[1], J. M. Orr[2], H. R. Smolker[2], F. Naaz[1], and M. T. Banich[2,3]

[1]Department of Psychological and Brain Sciences, University of Louisville, Louisville, KY 40292, USA, [2]The Institute of Cognitive Science, and [3]Department of Psychology and Neuroscience, University of Colorado Boulder, Boulder, CO 80309, USA

Address correspondence to Brendan E. Depue. Email: brendan.depue@louisville.edu

Abstract

Inhibitory control/regulation is critical to adapt behavior in accordance with changing environmental circumstances. Dysfunctional inhibitory regulation is ubiquitous in neurological and psychiatric populations. These populations exhibit dysfunction across psychological domains, including memory/thought, emotion/affect, and motor response. Although investigation examining inhibitory regulation within a single domain has begun outlining the basic neural mechanisms supporting regulation, it is unknown how the neural mechanisms of these domains interact. To investigate the organization of inhibitory neural networks within and across domains, we used neuroimaging to outline the functional and anatomical pathways that comprise inhibitory neural networks regulating cognitive, emotional, and motor processes. Networks were defined at the group level using an array of analyses to indicate their intrinsic pathway structure, which was subsequently assessed to determine how the pathways explained individual differences in behavior. Results reveal how neural networks underlying inhibitory regulation are organized both within and across domains, and indicate overlapping/common neural elements.

Key words: affect, cognition, inhibition, neuroimaging, prefrontal cortex

Introduction

Inhibitory control is critical to flexible adjustment of ongoing behavior according to changing environmental circumstances. The importance of inhibitory regulation is particularly evident in conditions where such control is dysfunctional, including both neurological (e.g., Parkinson's and Alzheimer's diseases; Amieva et al. 2004; van den Wildenberg et al. 2006) and psychiatric (e.g., attention-deficit hyperactivity, obsessive compulsive, mood, and substance use disorders; Murphy et al. 2000; Nigg et al. 2006; Page et al. 2009; Depue et al. 2010) conditions. Most striking is the broad manifestation of inhibitory dysfunction in multiple psychological domains, including cognitive, emotional, and motor processes (Murphy et al. 2000; Nigg et al. 2006; Page et al. 2009; Depue et al. 2010) within these populations. In view of this broad dysfunction in inhibitory regulation across disorders and domains, it is imperative to understand how the neural mechanisms underlying inhibitory regulation are organized in the neurologically intact brain.

Neuroimaging studies have focused mainly on the neural mechanisms involved in inhibitory regulation separately for cognitive, emotional, and motor processes, and have begun to outline the neural networks of each (Garavan et al. 1999; Ochsner et al. 2002; Eisenberger et al. 2003; Anderson et al. 2004; Aron et al. 2004; Phan et al. 2005; Aron and Poldrack 2006; Depue et al. 2007; Butler and James 2010; Congdon et al. 2010; Nowicka et al. 2011; Benoit and Anderson 2012; Sokol-Hessner et al. 2013). For instance, prefrontal regions engaged during inhibitory regulation of the

cognitive process of memory retrieval most prominently include the right middle and right inferior frontal gyri (rMFG and rIFG, respectively), which exerts inhibitory regulation of the hippocampus (HIP) to reduce retrieval and recollection (Anderson et al. 2004; Depue et al. 2007; Butler and James 2010; Nowicka et al. 2011; Benoit and Anderson 2012; Gagnepain et al. 2014). During inhibitory regulation of emotional reactivity, a number of prefrontal regions, including the right superior or right medial frontal gyri (rSFG and rmFG indicating medial), rIFG, rMFG, and the orbitofrontal cortex (OFC), downregulate amygdalar activity responsible for generating emotional and physiological responses (Ochsner et al. 2002; Eisenberger et al. 2003; Phan et al. 2005; Sokol-Hessner et al. 2013). During inhibitory regulation of motor responses, several different prefrontal regions, including the rIFG, rMFG, and anterior cingulate cortex or presupplementary motor area (ACC or pSMA), appear to initiate inhibition over subcortical output to the motor cortex via the subthalamic nucleus (STN), globus pallidus, and thalamus to stop motor responses (Garavan et al. 1999; Aron et al. 2004; Aron and Poldrack 2006; Congdon et al. 2010).

A common finding across the 3 domains is that the prefrontal cortex (PFC) putatively downregulates functional activity in and decreases communication between brain regions that underlie output to behavioral and cognitive effectors. More particularly, integration of the extant research literature suggests that the right lateral PFC (rLPFC), specifically the rMFG and rIFG, acts as a common neural element in the initiation of inhibitory regulation in each of these various psychological domains (Garavan et al. 1999; Eisenberger et al. 2003; Aron et al. 2004; Phan et al. 2005; Aron and Poldrack 2006; Depue et al. 2007; Butler and James 2010; Congdon et al. 2010; Nowicka et al. 2011; Benoit and Anderson 2012; Sokol-Hessner et al. 2013). In turn, a multitude of regions downstream of the PFC are involved in the cascade of inhibitory regulation depending on task requirements and responses [e.g., HIP, amygdala (AMY), and STN].

While the structure of the inhibitory networks for each domain is becoming clarified, (1) the extent to which these inhibitory networks, each of which involve the rLPFC, are distinct or share common neural elements, (2) which functional and anatomical principles they display, (3) their dependence on white-matter (WM) integrity, and (4) how these networks relate to behavior remains unknown. Unfortunately, these more complex questions about the structure and function of inhibitory networks have been difficult to answer, because research in cognitive neuroscience has primarily focused on the neural networks underlying inhibitory regulation within "single" psychological domains, that is cognitive (Anderson et al. 2004; Depue et al. 2007; Butler and James 2010; Nowicka et al. 2011; Benoit and Anderson 2012), emotional (Ochsner et al. 2002; Eisenberger et al. 2003; Phan et al. 2005; Sokol-Hessner et al. 2013), or motor (Garavan et al. 1999; Aron et al. 2004; Aron and Poldrack 2006; Congdon et al. 2010). A narrow empirical focus on single domains hinders attempts to determine the relationship between neural networks, if any, across multiple domains, and accordingly, how those networks and potential pathways may be organized. While different domains may be associated with distinct inhibitory networks, the brain can be considered an efficient processor (Ruppin et al. 1993) and, therefore, the evolution of neural networks underlying multiple domains of inhibitory regulation may also share common elements. Thus, understanding this organization and the degree to which neural networks overlap is an important step toward further treatment of neurological and psychiatric disorders.

While meta-analyses can provide some insights, and suggest that potential regions of interest (ROIs) within the PFC, what is needed to concretely address how inhibitory networks are organized, is to examine the neural correlates of inhibitory regulation over each psychological domain (i.e., cognitive, emotional, and motor) within the same individuals. Therefore, the current study utilized both group-level and individual difference analyses within and across 3 tasks assessing inhibitory regulation during cognitive, emotional, and motor behavior in the same individuals. By defining the general neural networks at the group level and isolating their constituent functional and anatomical neural elements that explain individual variation in inhibitory behavior, one can determine the organization of inhibitory regulation networks within each domain and subsequently, across multiple domains.

Our analysis utilized several procedures, including functional and anatomical criteria, to determine the neural network involved in inhibitory regulation within a given domain. First, we determined which brain regions exhibited regional activation for a task requiring inhibitory regulation in a standard group-level general linear model (GLM). Second, we determined which pairs of regions identified in the first procedure exhibited significant group-level seed-based functional connectivity. This procedure detected possible functional pathways between pairs of regions by estimating their coherence. Third, we determined which WM tracts' group-level integrity (fractional anisotropy, FA) was related to the functional pathways defined in the second procedure. This last procedure identified the possible anatomical pathways that predicted coherence of the functional pathways.

In summary, these analysis procedures provide the general neural networks associated with each domain of inhibitory regulation and subsequently, to increase power for 2 sets of neural predictors used to determine the degree to which they explain differences in inhibitory behavior across individuals. The sets of predictors include: (1) "functional pathways," which provide an individual's level of coherence between the neural regions intrinsic to each defined inhibitory network and (2) "anatomical pathways," which provide an individual's level of integrity of the WM tracts that related to the coherence of the functional pathways within each defined inhibitory network. Each functional and anatomical pathway within the sets of predictors was then used in feature/subset selection, robust regression, and mediation analyses to determine the best indicators of the individual differences in brain–behavior contributions both within and across different domains of inhibitory regulation. We predict that the neural networks underlying different domains of inhibitory regulation would exhibit common recruitment of MFG. However, this central hub will coordinate processing in distinct pathways or downstream brain regions dependent on the domain in which inhibitory regulation is exerted.

Materials and Methods

Behavioral Methods

Participants

A total of 24 healthy, right-handed individuals (10 females) were included in this study (mean age = 21.5, SD = 2.3 years), 3 subjects were excluded for incorrect diffusion tensor imaging (DTI) parameters, leaving a final N = 21. Participants were recruited through an online, CU-Boulder-based recruitment website, and were paid for their participation. Written informed consent was obtained prior to experimental sessions and all experimental protocols were approved by CU-Boulder's Institutional Review Board prior to data collection. Exclusion criteria included: psychiatric screening, left handedness, pregnancy, concussion, prior head injury in the last 30 days and metal intrinsic to the body.

Procedure

Three tasks were used to investigate inhibitory control over various psychological domains. To investigate inhibitory control over memory retrieval, we used the Think/No-Think task (TNT; Depue et al. 2007). To investigate inhibitory control over motor response, we used the Stop-signal task (SST; Chatham et al. 2012). To investigate inhibitory control over emotional reactivity, we used a variation of an emotion regulation paradigm (ER; Ochsner et al. 2002; Phan et al. 2005). Participants performed all 3 tasks in a single scanning session. The timing of the session is as follows: TNT scans (24 min), high-resolution scans (8 min), SST scans (10 min), DTI scans (12 min), ER scans (12 min), and resting-state scans (6 min). *Total time (72 min)*: High-resolution, DTI, and resting-state scans were conducted between tasks to allow for appropriate rest. Because the study aimed to investigate individual differences in a within-subject repeated-measures design which incorporated an emotional task, participants received the same task order (TNT, SST, and ER) with the emotional task performed last, to prevent carryover from heightened emotional responses.

Stimuli. TNT: Stimuli consisted of neutral faces and pictures taken from the International Affective Picture Series (IAPS; Lang et al. 1995). Neutral IAPS stimuli were selected for little to no positive or negative valence (neutral IAPS). *SST:* Stimuli consisted of simple arrows, circles, and squares informing individuals when respond to stimuli. *ER:* Stimuli consisted of negative valenced pictures taken from the IAPS (Lang et al. 1995) selected for a mean rate of negative valence.

TNT procedure. The task consisted of a training phase; participants learn 24 face–picture pairs, which are displayed for 4 s. Participants first viewed each pair, after all pairs were shown participants were shown only the faces and asked to select which of 2 pictures were originally paired with the face. Both of the 2 testing pictures came from the training phase, so that novelty of choice could not be used as a potential alternative cue for recognition. This procedure continued until the participant recognized the correct picture previously paired with a face with 97.5% accuracy (23 items) over all 24 pairs. In the experimental phase (fMRI scanning), participants saw the face for only 16 of the 24 pairs, half of these were relegated (counter-balanced for pairing and condition) to the Think condition, and half to the No-Think condition. An additional low-level fMRI Baseline including 8 novel faces was also presented. In all conditions, an experimental trial consisted of a face for 3.5 s, and then a 500-ms intertrial interval. The color of a border around the faces indicated the condition: Green for Think trials, red for No-Think trials, and yellow for low-level fMRI Baseline trials. In the Think condition, participants were told "Think of the picture previously associated with the face," whereas in the No-Think condition they were told "Do not to let the previously associated picture come into consciousness." During the low-level fMRI Baseline condition, participants were told to "Passively view the face." Within each condition (Think/No-Think/Baseline), participants also viewed faces 12 times (in-house scripts for a pseudorandom design order were used). Jittered fixation trials were interspersed in a pseudorandom order with a variable timing of 500–4000 ms. The 8 faces not shown in the experimental phase served as a 0-repetition behavioral baseline that assessed normal recollection accuracy. During the test phase, participants were shown each of the faces and told to write down a brief description of the picture originally associated with it. Behaviorally, both Think and No-Think trials were compared with Baseline trials to assess the degree to which the effect of exerting cognitive control over the stimuli had. An individual's inhibition index was computed by subtracting No-Think performance (percent accuracy) from baseline performance (percent accuracy). Correct performance in the Think and Baseline conditions equated to whether an individual remembered the item, whereas, in the No-Think condition, correct performance equates to whether an individual forgot the item. These data provided a behavioral performance index that could be used for regression analyses.

SST procedure. The Stop-signal task was implemented using the procedure and stimuli of Chatham et al. (2012). The task consisted of 240 two-choice reaction time (2CRT) trials, each involving a left or right pointing triangle. On 60 (i.e., 25%) of these trials, the imperative 2CRT stimulus was obscured by a stop-signal—a white box—following a variable stop-signal delay (SSD). Subjects were instructed that the stop-signal required all motor responses to be inhibited on that trial. The SSD was adjusted on a trial-by-trial basis using an adaptive algorithm; specifically, it was varied from its initial value of 100 ms according to each subject's performance. Following a failed stop-signal trial, the SSD was decreased from its previous value by 50 ms; following a successful stop-signal trial, the SSD was increased from its previous value by 50 ms. Both trial types consisted of either 2CRT or 2CRT plus SSD and a variable interstimulus interval (ISI) that equaled 2 s. Jittered fixation trials that presented 3 circles to incorporate a low-level fMRI baseline were interspersed in a pseudorandom order with a variable timing of 500–4000 ms (in-house scripts for a pseudorandom design order were used). The dependent measure, Stop-signal reaction time (SSRT), was calculated using the integration method; that is, SSRT was the *n*th percentile of each subject's correct Go signal RT distribution minus that subject's average SSD, where *n* is that subject's error rate on Stop-signal trials. An individual's SSRT provided a behavioral performance index that could be used for regression analyses.

ER procedure. The task procedure required participants to view negative IAPS pictures within 2 conditions: (1) (Suppress condition) participants are told to "Passively view the picture and remove yourself from any attached feeling" or (2) (Feel condition) participants are told to "View the picture and focus on the emotion it conveys." The task was a blocked design task with fixation trials at the end of each block to incorporate rest periods (60 s). Additional low-level fMRI baseline blocks, including 4 novel neutral pictures, repeated 4 times for 4 s were also presented at the beginning of the blocks to incorporate a more appropriate low-level baseline, in which participants simply viewed the neutral pictures. Twelve different negative IAPS pictures appeared in each condition (counter-balanced for condition) matched on valence and arousal. Each picture was repeated across 4 different blocks (48 s) per condition. A trial consists of a picture for 4 s, and then a 2-s intertrial interval. The color of a border around the pictures indicated the condition: Green for Feel trials and red for Suppress trials. Although relatively simple, this task has been used successfully in many ERs (13–14). Individuals also rated the 24 (12 per condition) and an additional 12 never previously viewed negative pictures on a Likert scale (1–7) at the end of the experiment. These subjective ratings provided behavioral measures in which Feel and Suppress trials were analyzed. Subjective ratings of both Feel and Suppress trials were compared with the Baseline items to assess whether invoking cognitive control had any increase and/or decrease of subjective ratings in each condition. An individual's inhibition index was computed by subtracting Suppress subjective ratings from baseline subjective

ratings. These data provided a behavioral performance index that could be used for regression analyses.

Neuroimaging Methods

Imaging Data Acquisition. *Structural.* All structural MRI images were acquired using a Siemens 3-T MAGNETOM Trio MR scanner located at the University of Colorado Boulder. A 12-channel head coil was used for radiofrequency transmission and reception. Foam padding was placed around the head, within the head coil, to limit head motion during the scan. Structural images were obtained via a T_1-weighted magnetization-prepared rapid gradient-echo sequence (MPRAGE) in 192 sagittal slices. Imaging parameters were as follows: echo time (TE) = 1.64 ms, repetition time (TR) = 2530 ms, flip angle = 7.0°, field of view (FoV) = 256 mm, and voxel size = 1.0 × 1.0 × 1.0 mm. Scan parameters were consistent for all imaging sessions associated with this study.

DTI. Structural connectivity was assessed with a diffusion-weighted scan (71 gradient directions; TR = 9600 ms; TE = 86 mm; GRAPPA parallel imaging factor 2; β-value = 1000 s/mm^2; FoV = 256 mm; 72 slices; 2 mm^3 isomorphic voxels; 7 β0 images).

Functional. Functional blood oxygenation level-dependent (BOLD) images were collected using gradient-echo T_2*-weighted echo-planar imaging (TR = 2000 ms; TE = 25 ms; 240 mm field of vision; 64 × 64 matrix; 31 axial slices, 3 mm slice thickness, 1 mm slice gap, 3.4 × 3.4 mm voxels; flip angle = 67°). Slices were oriented obliquely along the AC–PC line. The first 4 volumes from each run were discarded to allow for magnetic field equilibration.

Imaging Analyses. *DTI.* Diffusion-weighted images were processed using FSL's FDT toolbox (http://fsl.fmrib.ox.ac.uk/fsl/fslwiki/FDT; Behrens et al. 2003), and tract-based spatial statistics (TBSS; http://fsl.fmrib.ox.ac.uk/fsl/fslwiki/TBSS; Smith et al. 2006). Images were corrected for motion and eddy current distortions. A diffusion tensor model was fitted at each voxel, resulting in FA images. FA images for each participant were nonlinearly aligned to a 1 × 1 × 1 mm standard space FA template (Anderson et al. 2007). Aligned FA images were then skeletonized, and an average FA skeleton mask was created. WM tract ROIs were extracted from the JHU WM atlases available in FSL (Hua et al. 2008). WM ROIs were masked with the average FA skeleton, and the mean FA values were extracted for each participant from these ROIs. WM-ROIs were based on a priori determination of the most probable WM tracts connecting the functional ROIs from past studies investigating inhibitory control using the current tasks (Phan et al. 2005; Aron and Poldrack 2006; Depue et al. 2007). These included separate hemisphere masks (except the genu) for: superior and inferior longitudinal fasciculi (SLF/ILF), superior and inferior fronto-occipital fasciculi (sFOF/iFOF), the cingulum bundle (CB) which included the averaged FA values from the cingulum cingulate gyrus (CCG) and cingulum hippocampal part (CHp), the uncinate fasciculus (UNC), the external capsule (EC), anterior limb of the internal capsule (ALIC), posterior limb of the internal capsule (PLIC), superior region of the internal capsule (SCR), anterior region of the corona radiata (ACR), posterior region of the corona radiata (PCR), posterior thalamic radiation (PTR), and the genu of the corpus callosum (genu).

Functional. Image processing and data analysis were implemented using the FSL package (Analysis group, FMRIB, Oxford, UK, http://www.fmrib.ox.ac.uk/fsl/). Standard preprocessing was applied: MCFLIRT—linear slice-time correction/motion correction, BET—brain extraction, time-series prewhitening, high-pass filter (0.01 Hz), and registration and spatial normalization to the Montreal Neurological Institute (MNI) 152—T_1 2-mm template. Individual's functional images were first registered to their high-resolution MPRAGE scans via a 6-parameter linear registration, and the MPRAGE images were in turn registered to the MNI template via a 12-parameter nonlinear registration. These registrations were combined to align the functional images to the template. Functional images were resampled into the standard space with 2-mm isotropic voxels and were smoothed with a Gaussian kernel of 8-mm full-width at half-maximum.

Lower-level statistics were implemented in FEAT. Using multiple regression analysis, statistical maps representing the association between the observed time-series (e.g., BOLD signal) and one or a linear combination of regressors for each subject were constructed. Regressors in the main analyses were constructed from: (1) TNT (Think = T, No-Think = NT, cr = correct trials): T > NT, Tcr > NTcr, as well as each versus low-level fMRI baseline described in the procedure above (group-level SPMs were selected based on NTcr > Tcr), (2) ER (S = suppress, F = feel): S > F, as well as each versus low-level fMRI baseline described in the procedure above, and (3) SST (Sig = stop trials, No sig = CRT trials, cr = correct trials): Sig > No sig, Sigcr > No sigcr, as well as each versus. low-level fMRI baseline described in the procedure above (group-level SPMs were selected based on Sigcr > No sigcr). For each regressor, a double-gamma hemodynamic response function (HRF) was convolved with an event vector starting at the stimulus onset with a duration of: (1) TNT = 3.5 s, (2) ER = 4 s, and (3) SST = 2 s. Head motion (within rotation and translation) parameters (6-linear parameters: X, Y, and Z, for roll, pitch, and yaw, respectively) were included as confound regressors estimated by FSL's MCFLIRT. Errors were also included as a confound regressor. Contrasts of interest were formulated as linear combinations of the main regressors. Repeated-measures ANOVA and conjunction analyses utilized FSL's FEAT procedure for multisubject, multisession analyses (http://fsl.fmrib.ox.ac.uk/fsl/fslwiki/FEAT/UserGuide). We first used 3 separate lower-level models to motion correct to the mid-volume within task. Subsequently, a preliminary group-level fixed-effect model preserving within-subject variance was used to combine and register the 3 tasks' functional volumes together for each subject individually. Finally, a third-level mixed-effects model preserving within-subject variance, estimating between subjects variance (FLAME 1), and applying outlier de-weighting was used to combine and spatially normalize all subjects. The higher level models employed nonparametric permutation methods through FSL's randomize function (Nichols and Holmes 2002). One-sample *t*-tests for each contrast of interest were performed using the Threshold-Free Cluster Enhancement (TFCE) method, which detects clusters of contiguous voxels without first setting an arbitrary statistical cutoff (e.g., $Z > 2.58$), and controls the family-wise error (FWE) rate at $P < .05$. Each contrast underwent 5000 permutations. Randomize produces corrected 1-*p* maps, which we used to mask *t*-score maps for all figures and tables. Figures of statistical maps were created using FSLview.

Functional connectivity. Seed regions were based on ROIs selected if they passed 2 criteria: (1) The peak of activity from a standard whole-brain GLM passed the estimated threshold provided by FSL's TFCE and (2) was a priori ROIs defined by Phan et al. (2005), Aron and Poldrack (2006), and Depue et al. (2007). This approach requires that the tasks elicited activation during the current experiment, as well as, past experiments, thus increasing the likelihood of future replication. Subsequently, whole-brain

seed-based functional connectivity was performed by: Trimming functional data to remove 7 initial volumes and a first FSL FEAT model was run applying motion correction and high-pass filtering. Then, the first model's res4d and mean_func output are added together. From that output FSL's fslmeants utility extracted the average time course over 3 brain masks: ventricles, WM, and subject space whole brain, thresholded by fslmaths at 0.5 demeaned. A second FSL FEAT model was then run on the combined first model's res4d and mean_func output with the 3 demeaned time courses as explanatory variables (EVs). Subsequently, the res4d and mean_func output of the second model was added together, and FSL's fslmeants utility extracted the average demeaned time course over each of the experimental conditions (TNT = NTc > Baseline; ER = S > Baseline; SST = Sigc > Baseline) in subject space. This procedure uses the main condition of interest versus baseline to avoid independence issues. Finally, a third FSL FEAT model is then run on the combined res4d and mean_func output of the second model, with input EVs containing the masked demeaned condition time courses. After these 3 models were run per subject at the lower level, a higher level group model was then run in FSL FEAT. One-sample *t*-tests for each contrast of interest were performed using the TFCE method, which detects clusters of contiguous voxels without first setting an arbitrary statistical cutoff (e.g., $Z > 2.58$), and controls the FWE rate at $P < .05$. Each contrast underwent 5000 permutations. Randomize produces corrected 1-*p* maps, which we used to mask *t*-score maps for all figures and tables. Masks were then used to extract parameter estimates of functional connectivity at a 5-mm diameter standard space sphere surrounding peaks from selected ROIs, except for the STN, which was identified by MNI coordinates 10, −15, −5, which provides full STN coverage (Aron and Poldrack 2006). We then selected the peak STN voxel in an individual's subject space by applying the reverse of the transformation matrix used to register an individual to standard space. An individual's STN voxel was visually inspected against a high-resolution 7-T basal ganglia atlas (http://www.nitrc.org/projects/atag) to ensure localization. Because our ROI procedure centered a 5-mm diameter standard space sphere around peak activations, the spheres localized to the AMY extended into nonbrain tissue. Therefore, we extracted parameter estimates by applying a Harvard-Oxford bilateral mask. Figures of statistical maps were created using FSLview.

In summary, our full analysis procedure consisted of the following steps: (1) identify peaks of activity from a task-based GLM using the contrasts of TNT = NTcr > Tcr, ER = S > F, SST = Sigcr > No sigcr. If these regions also had been identified a priori in representative studies (Phan et al. 2005; Aron and Poldrack 2006; Depue et al. 2007), they were included in (2) seed-based functional connectivity analyses performed on the contrasts of TNT = NTc > Baseline; ER = S > Baseline; SST = Sigc > Baseline (using these different contrasts to avoid dependent analyses), (3) parameter estimates of functional connectivity were then extracted and analyzed in robust and multiple regression and mediation analysis to assess brain–behavior relationships.

Robust regression. Robust regression was conducted using Huber's method (Huber 1964) as an alternative to least squares regression to better estimate regression coefficients in the potential case where outliers were present in the data. To adequately adjust for our multiple comparisons and small sample size, we performed bootstrapping using 3000 iterations of Monte Carlo simulations to obtain upper and lower confidence intervals (CIs) of the beta estimates. Regressions were considered significant at the $P < 0.05$ two-tail level, provided the upper and lower CIs did not include zero. All *P*-values are adjusted for FDR as outlined in Benjamini and Hochberg (1995).

Multiple regression. To perform multiple regression, we used a two-stage procedure as outlined in Hastie et al. (2009). We first used penalized regression using LASSO (Tibshirani 1996) to perform subset variable/feature selection. Subsequently, because LASSO can over penalize highly collinear variables, we then performed an ordinary least squares (OLS) best model multiple regression on the subset of selected variables/features taken from LASSO to obtain beta estimates, regression coefficients, and determinants of explained variance. Finally, cross-validation was performed using leave-one-out (LOOCV) to provide measures of fit and cross-validated R^2. Regressions were considered significant at the $P < 0.05$ two-tail level. All *P*-values are adjusted for FDR as outlined in Benjamini and Hochberg (1995).

Mediation analyses. Mediation analyses were performed using the Preacher and Hayes (2004) method using the AMOS module for SPSS. Simple mediation analyses were run to examine any indirect effect of any independent variables on the relationship of other independent variables with the dependent variable. Again, to adequately adjust for our multiple comparisons and small sample size, we performed bootstrapping using 3000 iterations of Monte Carlo simulations to determine whether the indirect effect's beta estimate was different from zero. Indirect effects were considered significant at the $P < 0.05$ two-tail level. Partial versus full mediation was determined by establishing whether the beta estimate for the *c* pathway (relationship between the independent and dependent variables) was significantly different than zero.

Results

Behavior

To examine the neural mechanisms underlying "cognitive" inhibitory regulation, we used the TNT task (Anderson and Green 2001), which requires individuals to attempt to regulate memory retrieval of previously learned pairs of stimuli (behavioral measure: accuracy of attempted inhibition over retrieval compared with baseline memory). To assess "emotional" inhibitory regulation, we used an ER task (Ochsner et al. 2002; Phan et al. 2005), which requires individuals to attempt to regulate emotional reactivity to negative stimuli (behavioral measure: change in subjective ratings for attempted inhibition of emotional response compared with baseline ratings). To assess "motoric" inhibitory regulation, we used the SST (Chatham et al. 2012), which requires individuals to attempt to regulate motor responses by stopping an initiated button press cued by certain stimuli (behavioral measure: SSRT).

Consistent with previous results (Phan et al. 2005; Aron and Poldrack 2006; Depue et al. 2007), individuals were successful at: (1) reducing memory retrieval, when compared with baseline [$t_{(20)} = 2.07$, $P < 0.05$], (2) reducing their emotional reactivity to negative stimuli, when compared with baseline [$t_{(20)} = 2.59$, $P < 0.02$], and (3) inhibiting their motor responses [accuracy = 0.50 (0.006), GoRT = 442 (11.82), StopRT = 398 (8.17), SSD = 192 (16.23), SSRT = 228 (8.57); group average, standard error in parenthesis; for behavioral results, see Supplementary Material S1].

Neuroimaging

Inhibitory Regulation of Cognition (TNT Task)

Group-level GLM provided a set of peaks that were then used as seeds for functional connectivity. Results based on the overlap

of these 2 analyses indicated that upregulation of right anterior MFG (aMFG) was correlated with downregulation of the bilateral visual cortex and HIP (Fig. 1A). Increased integrity of the anatomical pathway between PFC and hippocampal regions as assessed by FA of the cingulum bundle (CB) predicted increased coherence of the right aMFG–HIP functional pathway ($R^2 = 0.40$, $F = 12.90$, $P = .002$; Fig. 1B). Better behavioral inhibitory regulation was associated with increased coherence of the aMFG–HIP functional pathway ($R^2 = 0.50$, $F = 18.74$, $P = 0.0004$) and increased integrity of the CB anatomical pathway ($R^2 = 0.20$, $F = 4.59$, $P = 0.04$).

Feature selection and regression indicated that the model best predicting behavior (an individual's ability to inhibit memory retrieval) included the functional pathway of right aMFG–HIP alone ($R^2 = 0.50$, $P = 0.0004$; Fig. 1C). However, analyses indicated that the CB anatomical pathway partially mediated the relationship between the right aMFG–HIP functional pathway and behavior ($P = 0.03$; Fig. 1D). These findings suggest that the neural network underlying successful inhibitory regulation of memory retrieval likely involves right aMFG regulation of hippocampal activity, and that this communication is facilitated by the integrity of the CB (for full TNT analyses, see Supplementary Material S2).

Inhibitory Regulation of Emotion (ER Task)

A group-level GLM provided a set of peaks that were then used as seeds for functional connectivity. Results based on the overlap of these 2 analyses indicated that upregulation of the right aMFG correlated with upregulation of the right lateral orbitofrontal cortex (OFC), which was correlated with downregulation of the bilateral AMY (Fig. 2A). Increased integrity of the anatomical pathway between PFC and ventral temporal/occipital regions as assessed by FA of the inferior fronto-occipital fasciculus (iFOF) predicted increased coherence of the right aMFG–OFC functional pathway ($R^2 = 0.34$, $F = 9.81$, $P = 0.006$; Fig. 2B). Increased integrity of the anatomical pathway between PFC and AMY/anterior temporal regions as assessed by FA of the uncinate fasciculus (UNC) predicted increased coherence of both the right aMFG–OFC and right OFC–AMY functional pathways ($R^2 = 0.39$, $F = 12.27$, $P = 0.002$; $R^2 = 0.23$, $F = 5.73$, $P = 0.03$, respectively). Increased coherence of the right aMFG–OFC and right OFC–AMY functional pathways both predicted better inhibitory regulation ($R^2 = 0.61$, $F = 32.85$, $P = 0.00001$; $R^2 = 0.34$, $F = 9.73$, $P = 0.006$, respectively). Better inhibitory regulation was also associated with increased integrity of the iFOF anatomical pathway ($R^2 = 0.30$, $F = 8.17$, $P = 0.003$).

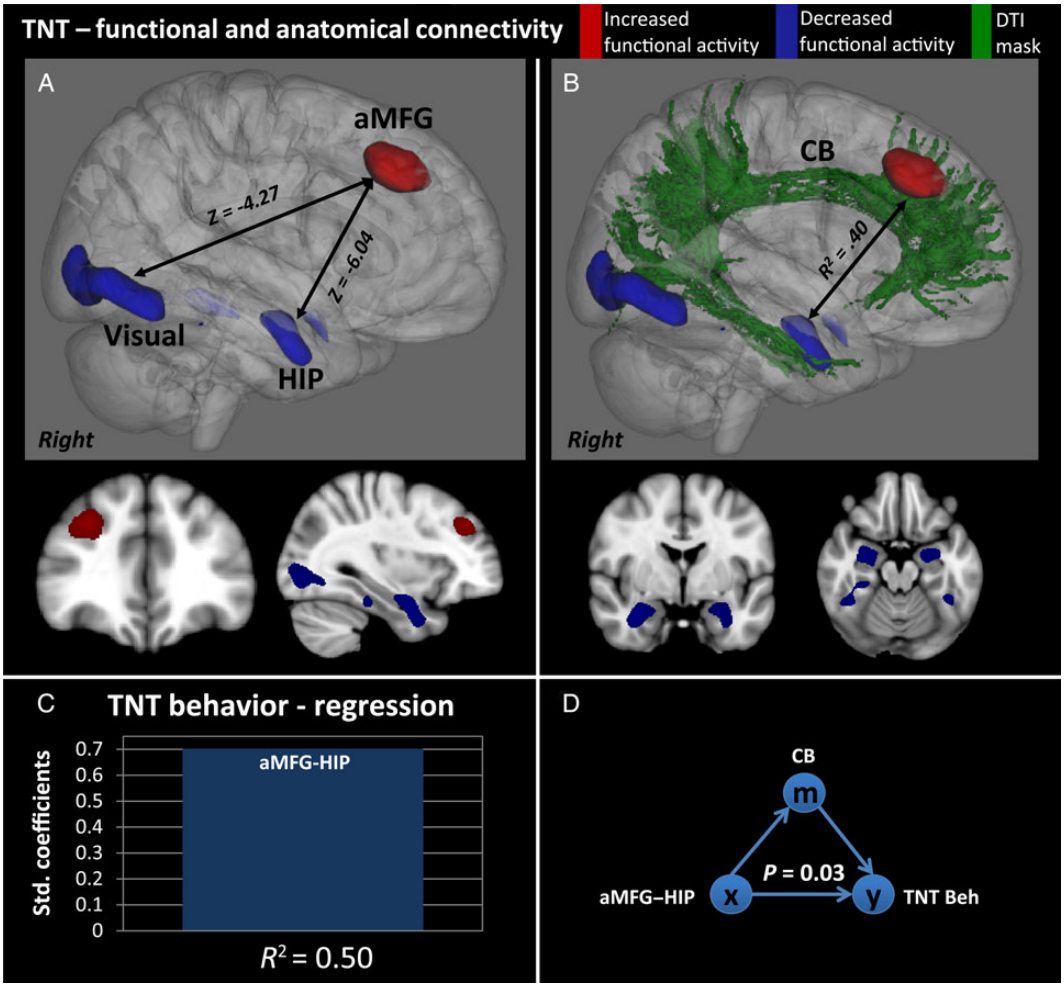

Figure 1. Functional and anatomical connectivity of the TNT ($N = 21$). (*A*) Significant brain regions of seed-based functional connectivity identified through the GLM. *Z* indicates the maximum functional connectivity parameter estimate (red/upregulation and blue/downregulation). (*B*) Significant WM tracts overlayed on the functional pathways, of which FA values predict the functional coherence. R^2 indicates the variance explained in the functional connectivity by the FA values from the CB. (*C*) Feature selection and multiple regression indicating the combination of predictors (aMFG–HIP) explaining the most variance in behavior (inhibition of memory retrieval). (*D*) Mediation analyses testing the indirect effect of a mediator (CB) on the relationship between the independent (aMFG–HIP) and dependent variables (inhibition of memory retrieval).

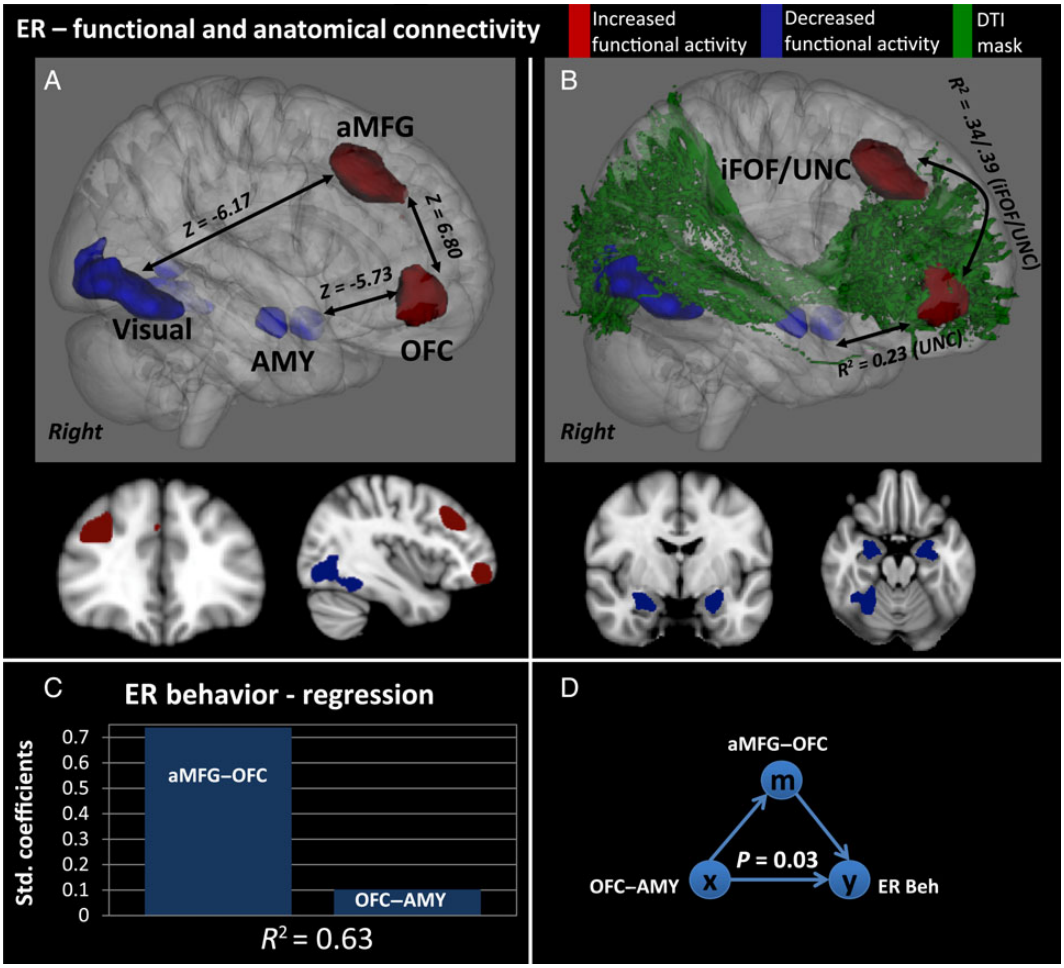

Figure 2. Functional and anatomical connectivity of the emotion regulation task (ER) ($N = 21$). (*A*) Significant brain regions of seed-based functional connectivity identified through the GLM. *Z* indicates the maximum functional connectivity parameter estimate (red/upregulation and blue/downregulation). (*B*) Significant WM tracts overlayed on the functional pathways, of which FA values predict the functional coherence. R^2 indicates the variance explained in the functional connectivity by the FA values from the iFOF and UNC. (*C*) Feature selection and multiple regression indicating the combination of predictors (aMFG–OFC and OFC–AMY) explaining the most variance in behavior (inhibition of emotional response). (*D*) Mediation analyses testing the indirect effect of a mediator (aMFG–OFC) on the relationship between the independent (OFC–AMY) and dependent variables (inhibition of emotional response).

Feature selection and multiple regression indicated that the model best predicting behavior (an individual's ability to inhibit emotional reactivity) included both functional pathways (aMFG–OFC and OFC–AMY; $R^2 = 0.63$, $P = 0.0001$; Fig. 2*C*). Analyses indicated that the coherence of the right aMFG–OFC functional pathway partially mediated the relationship between the right OFC–AMY functional pathway and behavior ($P = 0.03$; Fig. 2*D*). These findings indicate that the neural network underlying successful inhibitory regulation of emotional reactivity likely involves communication between the right aMFG and right OFC to regulate amygdalar activity, which appears to be facilitated by the integrity of the iFOF and UNC (for full ER analyses, see Supplementary Material S3).

Inhibitory Regulation of Motor (SST Task)

A group-level GLM provided a set of peaks that were then used as seeds for functional connectivity. Results based on the overlap of these 2 analyses indicated that (1) upregulation of the right posterior MFG (pMFG) was correlated with upregulation of the right IFG and ACC, (2) upregulation of the right IFG was correlated with upregulation of the STN and ACC (Fig. 3*A*). Increased integrity of the anatomical pathway between PFC and subcortical/thalamic regions as assessed by FA of anterior limb of the internal capsule (ALIC) predicted increased coherence of the right pMFG–ACC and right IFG–STN functional pathway ($R^2 = 0.20$, $F = 4.74$, $P = 0.04$; $R^2 = 0.20$, $F = 4.44$, $P = 0.04$, respectively; Fig. 3*B*). Increased coherence of the right pMFG–IFG, pMFG–ACC, and right IFG–STN functional pathways all predicted better inhibitory regulation ($R^2 = 0.21$, $F = 4.92$, $P = 0.04$; $R^2 = 0.20$, $F = 4.77$, $P = 0.04$; $R^2 = 0.32$, $F = 8.97$, $P = 0.007$, respectively).

Feature selection and multiple regression indicated that the model best predicting behavior (an individual's ability to inhibit motor response) included the functional pathways of right pMFG–IFG, right pMFG–ACC, and right IFG–STN ($R^2 = 0.44$, $P = 0.001$; Fig. 3*C*). Analyses indicated that the coherence of the right IFG–STN functional pathway partially mediated both relationships between the right pMFG–ACC and right pMFG–IFG functional pathways and behavior ($P = 0.03$ and 0.04, respectively; Fig. 3*D*). These findings suggest that the neural network underlying successful inhibitory regulation of motor response likely involves: Communication between the right pMFG, right IFG, and ACC to regulate the STN, which in turn is responsible for

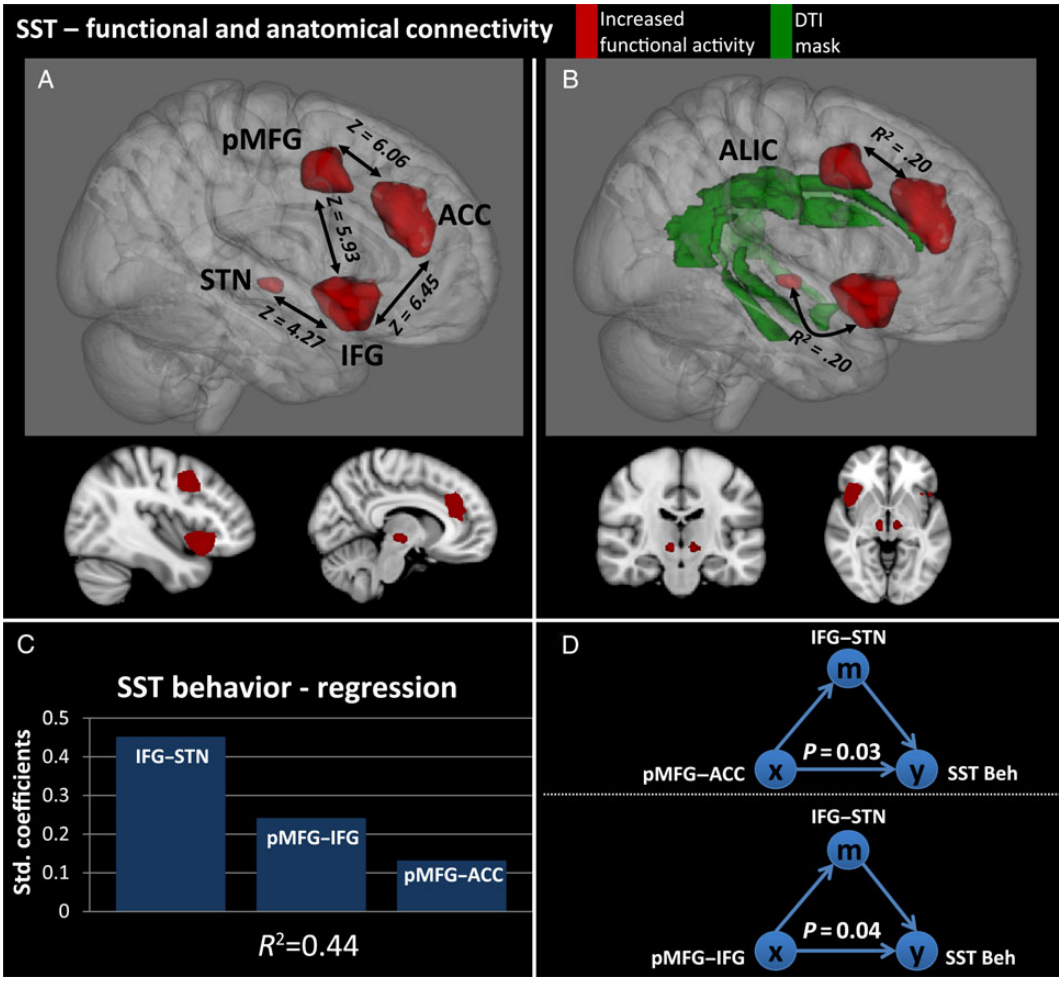

Figure 3. Functional and anatomical connectivity of the SST (N = 21). (*A*) Significant brain regions of seed-based functional connectivity identified through the GLM. *Z* indicates the maximum functional connectivity parameter estimate (red/upregulation and blue/downregulation). (*B*) Significant WM tracts overlayed on the functional pathways, of which FA values predict the functional coherence. R^2 indicates the variance explained in the functional connectivity by the FA values from the ALIC. (*C*) Feature selection and multiple regression indicating the combination of predictors (IFG–STN, pMFG–IFG, and pMFG–ACC) explaining the most variance in behavior (inhibition of motor response). (*D*) Mediation analyses testing the indirect effect of a mediator (IFG–STN) on the relationship between both independent (pMFG–ACC and pMFG–IFG) and dependent variables (inhibition of motor response).

initiating a neural cascade of inhibition to stop motor response, via the pallidum and thalamus (for full SST analyses, see Supplementary Material S4).

Across Task

Correlations across behavioral measures indicated that inhibitory regulation was only correlated across individuals between the TNT and ER tasks ($R^2 = 0.33$, $F = 9.5$, $P = 0.006$; see Supplementary Material S5). Functional pathway predictors that explained the most variance in single task behavior [aMFG–HIP (TNT), aMFG–OFC (ER), and IFG–STN (SST)] were highly correlated across task: aMFG–HIP (TNT) correlated with both aMFG–OFC (ER; $R^2 = 0.25$, $F = 6.39$, $P = 0.02$) and IFG–STN (SST; $R^2 = 0.38$, $F = 11.45$, $P = 0.003$), aMFG–OFC (ER) correlated with pMFG–IFG (SST; $R^2 = 0.25$, $F = 6.33$, $P = 0.02$), and OFC–AMY (ER) correlated with IFG–STN (SST; $R^2 = 0.39$, $F = 12.32$, $P = 0.002$; Fig. 4A; see Supplementary Material S5). Anatomical pathway predictors that contributed to each of the single task's described neural networks [CB (TNT), iFOF/UNC (ER), and ALIC (SST)] also were correlated across task. The CB (TNT) correlated with the iFOF (ER) and the ALIC (SST; $R^2 = 0.64$, $F = 33.76$, $P = 0.00001$; $R^2 = 0.37$, $F = 11.35$, $P = 0.003$, respectively). The UNC (ER) correlated with the iFOF (ER) and the ALIC (SST; $R^2 = 0.31$, $F = 8.52$, $P = 0.009$; $R^2 = 0.57$, $F = 25.51$, $P = 0.0001$, respectively). Finally, the iFOF (ER) correlated with the ALIC (SST; $R^2 = 0.60$, $F = 27.95$, $P = 0.00001$; see Supplementary Material S5). Repeated-measures ANOVA and conjunction analyses on whole-brain functional activation across the 3 tasks indicated that only the right MFG and right angular gyrus were consistently activated across all 3 tasks (Fig. 4B; see Supplementary Material S5). However, because only the right MFG exhibited functional connectivity in the 3 individual tasks, we focused on that region.

Because the pathways correlated highly across task, we determined whether they exhibited specificity to the inhibitory regulation task in which they were defined. To do so, we examined each of the functional and anatomical pathways in relation to behavioral performance in the other 2 tasks. Of the 11 functional and anatomical pathways, only the pathway of aMFG–HIP exhibited a trend toward significance for predicting behavior in the ER task ($R^2 = 0.14$, $F = 3.15$, $P = 0.09$), suggesting that the pathways are relatively specific to the inhibitory regulation task in which they were defined, but that the coherence and integrity of the pathways is related across task within individuals (for full across task analyses, see Supplementary Material S5).

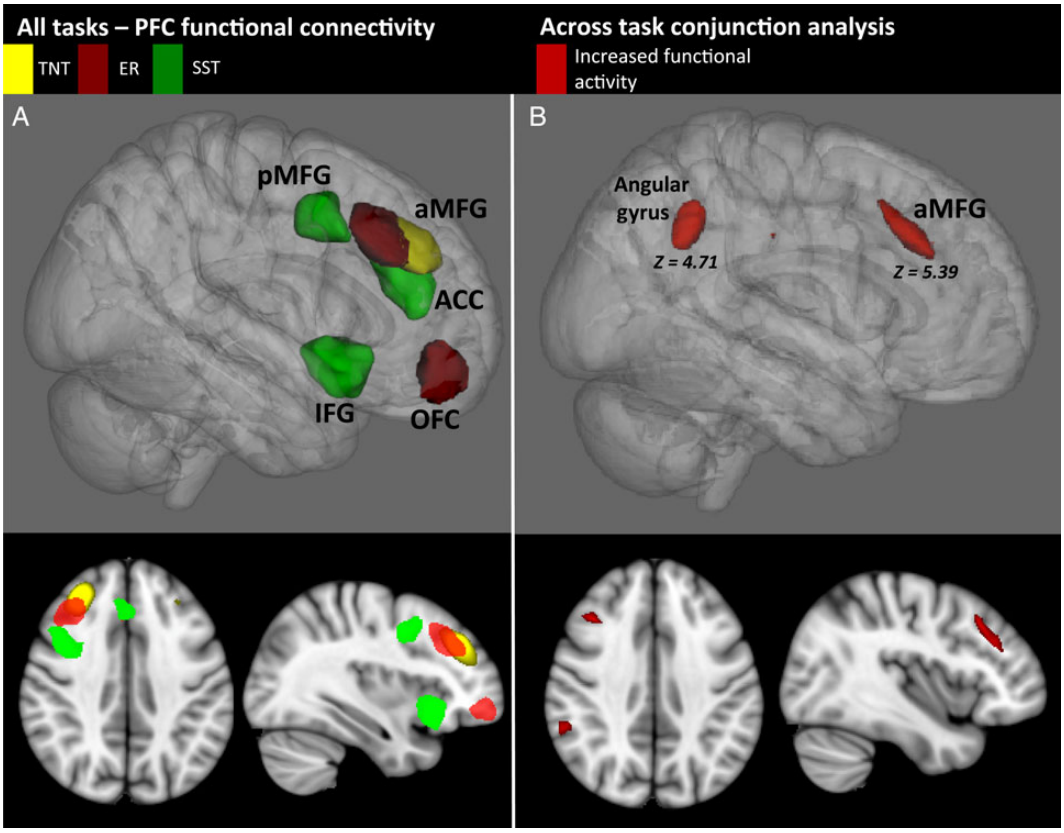

Figure 4. (*A*) Significant prefrontal brain regions of seed-based functional connectivity identified through the GLM within individual tasks [Think/No-Think (TNT) = yellow, Emotion Regulation (ER) = red, and Stop-signal (SST) = green)] ($N = 21$). (*B*) Repeated-measures ANOVA and conjunction analysis of functional activation across the 3 tasks indicating common activation of the angular gyrus and aMFG. Z indicates the peak functional activity parameter estimate across tasks.

Moreover, although the majority of the prefrontal components of the functional pathway predictors appear to be spatially or anatomically distinct for each type of inhibitory regulation, a region within the right MFG and its connectivity appear to overlap across tasks.

Discussion

The current study provides a detailed account of the neural networks underlying inhibitory regulation of cognitive, affective, and motor processes by examining 3 divergent inhibitory tasks performed by the same individuals. Using structural and functional neuroimaging, we demonstrate the overarching organization of 3 distinct inhibitory neural networks, each of which incorporate functional pathways that exhibit coherence between pairs of brain regions and anatomical pathways that predict the coherence of the functional pathways, thus indicating the interconnectivity of brain regions within the networks. These converging pathways have robust explanatory power in predicting brain–behavior relationships underlying inhibitory regulation, evidenced by the degree of variance explained (44%–63%) in the regression models for each of the 3 different inhibitory networks. We subsequently showed that each inhibitory domain's set of pathways highly correlated across task, but only predicted behavior with the task in which they were defined, indicating their specificity. These findings indicate strong relationships between the functional and anatomical pathways underlying inhibitory regulation across the 3 psychological domains. Finally, we determined that a common brain region, the right MFG, is recruited across all 3 inhibitory regulation tasks. Individual regions of the right MFG indicated peaks of localization occurring along a gradient from more posterior regions involved in motor inhibition and more anterior ones in emotional and cognitive inhibition.

The neural network responsible for inhibitory regulation over memory retrieval predominantly involves the pathway that allows modulation of the HIP by the right anterior MFG (Fig. 1*A*), which accounted for a high degree of behavioral variance ($R^2 = 0.50$). This pathway is consistent with the current fMRI literature, which also suggests modulatory effects of the MFG over the HIP (Anderson et al. 2004; Depue et al. 2007; Butler and James 2010; Benoit and Anderson 2012). Here, we also provide the first empirical evidence that the CB, the WM tract connecting the aMFG–HIP pathway (Schmahmann and Pandya 2006), plays a critical role in this network, as the CB's integrity correlated with inhibition regulation of memory retrieval, and was highly predictive of coherence of the aMFG–HIP pathway ($R^2 = 0.40$; Fig. 1*B*). Indicating an intrinsic relation between function, structure, and behavior, integrity of the CB was found to partially mediate the relation between the aMFG–HIP pathway and cognitive inhibition.

The neural network responsible for inhibitory regulation of emotional reactivity involves at least 2 pathways: right aMFG with the OFC, and the right OFC with the AMY (Fig. 2*A*), which contributed independent variance in a multiple regression predicting inhibitory regulation of emotion ($R^2 = 0.63$). This network may function hierarchically, with the aMFG modulating the lateral OFC's inhibitory regulation of the AMY, which is consistent with the current literature (Eisenberger et al. 2003; Phan et al. 2005; Sokol-Hessner et al. 2013). We extend the functional and anatomical characterization of this network by demonstrating that iFOF and UNC, the WM tracts connecting the aMFG–OFC

and OFC–AMY pathways (Martino et al. 2010; Von Der Heide et al. 2013), respectively, predicted their coherence ($R^2 = 0.34$ and 0.23, respectively; Fig. 2B). Indicating that coordination between these 2 pathways is likely, the aMFG–OFC partially mediated the influence of the OFC–AMY with inhibitory behavior.

The neural network underlying inhibitory regulation of motor response involves at least 3 pathways: right pMFG with the right IFG, right pMFG with the ACC, and the right IFG with the STN (Fig. 3A), each of which contributed independent variance in a multiple regression predicting motor inhibition ($R^2 = 0.44$). Research indicates that the IFG and/or the ACC signal the STN to initiate a cascade of neural inhibition via the pallidum, resulting in decreased information flow to the thalamus and subsequently to the motor cortex to terminate a motor response (Aron et al. 2004; Aron and Poldrack 2006). While our results reflect this general circuitry, our data further suggest that this neural network may function in a similar fashion as outlined for the inhibitory regulation of emotion network above: where hierarchical influence of the pMFG acts via the IFG and the ACC. This is supported by the fact that the influence on motor inhibition by both the pMFG–IFG and pMFG–ACC pathways was partially mediated by the IFG–STN pathway, again suggesting coordination between the former 2 pathways. We further suggest that the pMFG–ACC pathway has an additive effect by (i) monitoring the success of motor stopping and (ii) providing additional neural support/feedback. Providing anatomical support for this network, we show that increased integrity of the ALIC, which connects the IFG–STN pathway (Nieuwenhuys, et al. 1988), the largest mediating predictor of the network, is related to its coherence ($R^2 = 0.20$; Fig. 3B).

Comparing behavioral performance and each of the sets of functional and anatomical pathway predictors *across* task indicated a high degree of association between pathways of the 3 domains' inhibitory regulation. Behavioral performance correlated between the TNT and ER tasks ($R^2 = 0.33$), but not the SST. This may reflect an increase in the relatedness of behavioral performance measures between inhibitory tasks that can be considered cognitive (e.g., TNT and ER) when compared with inhibitory tasks that are more behavioral (e.g., SST) in nature. However, the functional and anatomical pathways between all 3 tasks were highly related. The functional (aMFG–HIP, aMFG–OFC, and IFG–STN) and anatomical (CB, iFOF, UNC, and ALIC) pathways that accounted for the most explained variance in behavioral performance for each of the tasks accounted for a large degree of variance in one another's functional coherence (25–40%) and in one another's anatomical integrity (30–64%), respectively.

The relatedness among the 3 domain networks found in our data raises the question of how these networks are neurally coordinated. A striking finding across all 3 of the above networks indicates the recruitment of a common region of the right MFG, suggesting a prominent role during inhibitory regulation. Individually, the tasks exhibited right MFG recruitment during inhibitory regulation of memory retrieval and emotional reactivity localized to "anterior" MFG, whereas inhibitory regulation of motor response recruited a distinct but more "posterior" region of the MFG. This anterior–posterior delineation of the MFG in our data is consistent with several prominent theoretical views of PFC function. First, there is evidence indicating that inhibition can be segmented into behavioral and cognitive components (Harnishfeger 1995; Aron 2007). Second, a major synthesis of PFC function suggests that the organization of the PFC has evolved to exhibit a gradient of increasing abstraction (Badre 2008; Badre and D'Esposito 2009; Christoff et al. 2009) from posterior to anterior regions of the PFC (e.g., from concrete, motor functions to abstract, cognitive processes). Although specific evidence for the functional organization of the MFG is sparse relative to the PFC in general [however, see Nee and Brown (2012)], our data are consistent with a gradient of abstraction view, where the pMFG represents behavioral/motor information and the aMFG is involved with cognitive/affective representations.

In view of the fact that the right MFG is common to the 3 networks, we suggest that it resides at the top of a functional hierarchy of regions in each inhibitory network. Its position at the top of hierarchies suggests that its function incorporates a working memory process that enables it to maintain and update goal-related information, which is highly consistent with literature concerning its anatomical and functional connectivity (Goldman-Rakic et al. 1984; Morris et al. 1999; Miller and Cohen 2001; D'Ardenne et al. 2012). In the case of inhibitory regulation of memory retrieval, the network has a single hierarchical level, possibly because both maintenance and updating of the task goal and modulation of the HIP is accomplished by the same region (MFG), due to its direct anatomical connections (i.e., CB). During inhibitory regulation of emotional reactivity and/or motor response, higher-order maintenance and updating of task goals would be performed by MFG, whereas modulation of the AMY or STN (downstream effectors) is performed by an intermediary region (OFC and IFG, respectively) that exhibits direct anatomical connectivity (i.e., UNC and ALIC, respectively), increasing the hierarchical nature of these neural networks. Therefore, we suggest that a central role of the MFG during inhibitory regulation is to: (1) update and maintain a task goal or representation, and then subsequently (2) influence the activity of other network regions to accomplish the goal. Supporting this view, the 3 functional pathways involving the MFG that accounted for the most explained variance in behavioral performance in each of the tasks all correlated with performance on a working memory task requiring both updating and maintenance (see Supplementary Material S6). Thus, the role of MFG during inhibitory regulation is more parsimonious with a view of it performing working memory and goal-oriented operations than to strictly perform neural inhibition over other brain regions.

Recent literature discusses multiple viewpoints of inhibitory control, ranging from its necessity to its superfluousness. However, this debate is complicated by the multitude of inhibitory definitions in such arguments. Definitions include, behavioral inhibition (reduction in behavior), cognitive inhibition (the mind's capacity to tune down irrelevant processing), and neural inhibition (the physical mechanism by which neurons signal; i.e., GABAergic interneurons), to name a few. While the question of whether inhibition is necessary lies outside the scope of this article, we refer the reader to recent research that presents a variety of differing views. As done quite elegantly in a recent paper (Erika-Florence et al. 2014), the authors discuss a computational perspective for the role of top-down potentiation (inducing local collateral inhibition), rather than top-down inhibition, that renders behavioral inhibition obsolete. However, Aron and colleagues (Cai et al. 2011) recently present strong evidence for behavioral inhibition, by indicating reductions in effector muscle motor-evoked potentials below resting rates. While the evidence for both cases is strong and may seem at odds, our previous work provides a framework that helps to reconcile these 2 perspectives (Munakata et al. 2011; Depue 2012). This framework suggests that different types of inhibition may emanate from the PFC in both a "global and directed" as well as an "indirect and local" fashion. Briefly, the former taking form of long-range excitatory projections from the PFC synapsing on distinct inhibitory cell populations or gating mechanisms in nonneocortical or subcortical

brain regions in order to decrease their activity or output (e.g., fear extinction). While the latter involves cortical representations competing for expression, which is resolved through lateral inhibition to amplify the selected representation (e.g., selection and attention). While we do not ascribe to the notion that the rLPFC contains discrete units or modules associated with inhibition, the current study indicates that regions within the rLPFC may serve to regulate a nonneocortical or subcortical region's output to reduce unwanted behavior or cognition.

One distinct feature highly apparent in our data, as well as across a majority of neuroimaging studies investigating inhibitory regulation, is the predominance in the recruitment of the "right" hemisphere (Garavan et al. 1999; Eisenberger et al. 2003; Aron et al. 2004; Phan et al. 2005; Aron and Poldrack 2006; Depue et al. 2007; Butler and James 2010; Congdon et al. 2010; Nowicka et al. 2011; Benoit and Anderson 2012; Sokol-Hessner et al. 2013). To our knowledge, no formal theoretical view regarding the neural networks underlying inhibitory regulation account for these findings. Research suggests a relative difference in processing of the right versus left hemisphere, with the right showing predominance in (1) early development (Chiron et al. 1997), (2) object-based recognition and spatial processing when compared with language (Gauthier et al. 1999), (3) processing stimuli in a global or holistic manner when compared with local or feature-based representation (Fink et al. 1997), (4) encoding and integrating the temporal duration of events (McKibbin et al. 2003), (5) withdrawal when compared with approach behavior (Davidson et al. 1990), (6) generating negative when compared with positive emotion (Davidson 1992), and (7) sensitivity to faces, body posture, and prosody especially in the context of threat (Ohman 2002; Sander et al. 2005; De Gelder 2006). Taken together, these findings suggest that the right hemisphere may provide a relatively quick snapshot and global representation of the current environmental context. This global representation would contain crude yet rapidly processed information about potentially threatening stimuli and, if so perceived, would initiate negative affect (e.g., fear) and withdrawal. Under such circumstances, being able to apply inhibitory regulation of (1) selection or interruption of already-initiated motor programs, (2) emotional reactivity to reduce behavioral freezing or panic, and subsequently (3) intrusive memories may increase survival. Because inhibitory regulation under potentially threatening circumstances would be required early in life, throughout evolutionary adaptation, inhibitory regulation may have been selected for right hemispheric dominance due to its earlier developmental trajectory. And given the multiple behavioral systems requiring inhibitory regulation during such events, prefrontal coordination (e.g., via MFG) would be required to assure synchronized processing across domains.

In all, the current research indicates detailed functional and anatomical neural networks for various psychological domains of inhibitory regulation. Furthermore, we emphasize the potential higher-order coordinating role of the right MFG, which putatively initiates inhibitory regulation across the 3 domain networks by updating and maintaining important working memory representations. Defining neuroanatomical models contributing to inhibitory regulation is critical to understanding and treating neurological and psychiatric diseases affected by inadequate self-regulation.

Supplementary Material

Supplementary material can be found at: http://www.cercor.oxfordjournals.org/.

Funding

This work was supported by NIMH grant # P50–079485.

Notes

We thank the anonymous reviewers for extremely thoughtful comments, which improved the manuscript tremendously. *Conflict of Interest*: None declared.

References

Amieva H, Phillips LH, Della Sala S, Henry JD. 2004. Inhibitory functioning in Alzheimer's disease. Brain. 1275:949–964.

Anderson JL, Jenkinson M, Smith S, Andersson J. 2007. Non-linear optimization. FMRIB technical report. TR07JA:1.

Anderson MC, Green C. 2001. Suppressing unwanted memories by executive control. Nature. 410:366–369.

Anderson MC, Ochsner KN, Kuhl B. 2004. Neural systems underlying the suppression of unwanted memories. Science. 303:232–235.

Aron AR. 2007. The neural basis of inhibition in cognitive control. Neuroscientist. 133:214–228.

Aron AR, Poldrack RA. 2006. Cortical and subcortical contributions to stop signal response inhibition: role of the subthalamic nucleus. J Neurosci. 26:2424–2433.

Aron AR, Robbins TW, Poldrack RA. 2004. Inhibition and the right inferior frontal cortex trends in cognitive. Sciences. 84: 170–177.

Badre D. 2008. Cognitive control, hierarchy, and the rostro–caudal organization of the frontal lobes. Trends Cogn Sci. 125: 193–200.

Badre D, D'Esposito M. 2009. Is the rostro-caudal axis of the frontal lobe hierarchical? Nat Rev Neurosci. 109:659–669.

Behrens TEJ, Woolrich MW, Jenkinson M, Johansen-Berg H, Nunes RG, Clare S, Smith SM. 2003. Characterization and propagation of uncertainty in diffusion-weighted MR imaging. Magn Reson Med. 505:1077–1088.

Benjamini Y, Hochberg Y. 1995. Controlling the false discovery rate: a practical and powerful approach to multiple testing. J R Stat Soc B. 289–300.

Benoit RG, Anderson MC. 2012. Opposing mechanisms support the voluntary forgetting of unwanted memories. Neuron. 762:450–460.

Butler AJ, James KH. 2010. The neural correlates of attempting to suppress negative versus neutral memories. Cogn Affect Behav Neurosci. 10:182–194.

Cai W, Oldenkamp CL, Aron AR. 2011. A proactive mechanism for selective suppression of response tendencies. J Neurosci. 31:5965–5969.

Chatham CH, Claus ED, Kim A, Curran T, Banich MT. 2012. Cognitive control reflects context monitoring, not motoric stopping, in response inhibition. PLoS ONE. 72:e31546.

Chiron C, Jambaque I, Nabbout R, Lounes R, Syrota A, Dulac O. 1997. The right brain hemisphere is dominant in human infants. Brain. 120:1057–1065.

Christoff K, Keramatian K, Gordon AM, Smith R, Mädler B. 2009. Prefrontal organization of cognitive control according to levels of abstraction. Brain Res. 1286:94–105.

Congdon E, Mumford JA, Cohen JR, Galvan A, Aron AR, Xue G, Poldrack RA. 2010. Engagement of large-scale networks is related to individual differences in inhibitory control. NeuroImage. 532:653–663.

D'Ardenne K, Eshel N, Luka J, Lenartowicz A, Nystrom LE, Cohen JD. 2012. Role of prefrontal cortex and the midbrain dopamine system in working memory updating. Proc Natl Acad Sci. 10949:19900–19909.

Davidson RJ. 1992. Emotion and affective style: hemispheric substrates. Psychol Sci. 31:39–43.

Davidson RJ, Ekman P, Saron CD, Senulis JA, Friesen WV. 1990. Approach-withdrawal and cerebral asymmetry: emotional expression and brain physiology. J Pers Soc Psychol. 582: 330–341.

De Gelder B. 2006. Towards the neurobiology of emotional body language. Nat Rev Neurosci. 73:242–249.

Depue BE. 2012. A neuroanatomical model of prefrontal inhibitory modulation of memory retrieval. Neurosci Biobehav Rev. 36:1382–1399.

Depue BE, Burgess GC, Willcutt EG, Ruzic L, Banich MT. 2010. Inhibitory control of memory retrieval and motor processing associated with the right lateral prefrontal cortex: evidence from deficits in individuals with ADHD. Neuropsychologia. 48:3909–3917.

Depue BE, Curran T, Banich MT. 2007. The prefrontal cortex orchestrates the suppression of emotional memories via a two-phase process. Science. 317:215–219.

Eisenberger NI, Lieberman MD, Williams K. 2003. Does rejection hurt? An fMRI study of social exclusion. Science. 302:290–292.

Erika-Florence M, Leech R, Hampshire A. 2014. A functional network perspective on response inhibition and attentional control. Nat Commun. 5:1–11.

Fink GR, Halligan PW, Marshall JC, Frith CD, Frackowiak RS, Dolan RJ. 1997. Neural mechanisms involved in the processing of global and local aspects of hierarchically organized visual stimuli. Brain. 120:1779–1791.

Gagnepain P, Henson RN, Anderson MC. 2014. Suppressing unwanted memories reduces their unconscious influence via targeted cortical inhibition. Proc Natl Acad Sci USA. 111.13:E1310–E1319.

Garavan H, Ross TJ, Stein EA. 1999. Right hemisphere dominance for inhibitory control: an event-related functional MRI study. Proc Natl Acad Sci USA. 96:8301–8306.

Gauthier I, Tarr MJ, Anderson AW, Skudlarski P, Gore JC. 1999. Activation of the middle fusiform "face area" increases with expertise in recognizing novel objects. Nat Neurosci. 2:568–573.

Goldman-Rakic PS, Selemon LD, Schwartz ML. 1984. Dual pathways connecting the dorsolateral prefrontal cortex with the hippocampal formation and parahippocampal cortex in the rhesus monkey. Neuroscience. 12:719–743.

Harnishfeger K. 1995. Development of cognitive inhibition. In: Dempster F, Brainerd C, editors. Interference and inhibition in cognition. San Diego: Academic.

Hastie T, Tibshirani R, Friedman J. 2009. Linear methods for regression. New York: Springer. p. 43–99.

Hua K, Zhang J, Wakana S, Jiang H, Li X, Reich DS, Mori S. 2008. Tract probability maps in stereotaxic spaces: analyses of white matter anatomy and tract-specific quantification. Neuroimage. 391:336–347.

Huber PJ. 1964. Robust estimation of a location parameter. Ann Math Stat. 351:73–101.

Lang PJ, Bradley MM, Cuthbert BN. 1995. The International Affective Picture System IAPS. Gainesville: University of Florida, Center for Research in Psychophysiology.

Martino J, Brogna C, Robles SG, Vergani F, Duffau H. 2010. Anatomic dissection of the inferior fronto-occipital fasciculus revisited in the lights of brain stimulation data. Cortex. 46:691–699.

McKibbin K, Elias LJ, Saucier DM, Engebregston D. 2003. Right-hemispheric dominance for processing extended non-linguistic frequency transitions. Brain Cogn. 53: 322–326.

Miller EK, Cohen JD. 2001. An integrative theory of prefrontal cortex function. Ann Rev Neurosci. 241:167–202.

Morris RE, Pandya DN, Petrides M. 1999. Fiber system linking the mid-dorsolateral frontal cortex with the retrosplenial/presubicular region in the rhesus monkey. J Comp Neurol. 407:183–192.

Munakata Y, Herd SA, Chatham CH, Depue BE, Banich MT, O'Reilly RC. 2011. A unified framework for inhibitory control. Trends Cogn Sci. 15:453–459.

Murphy FC, Sahakian BJ, Rubinsztein JS, Michael A, Rogers RD, Robbins TW, Paykel ES. 2000. Emotional bias and inhibitory control processes in mania and depression. Psychol Med. 29:1307–1321.

Nee DE, Brown JW. 2012. Rostral–caudal gradients of abstraction revealed by multi-variate pattern analysis of working memory. Neuroimage. 63:1285–1294.

Nichols TE, Holmes AP. 2002. Nonparametric permutation tests for functional neuroimaging: a primer with examples. Hum Brain Mapp. 151:1–25.

Nieuwenhuys R, Voogd J, van Huijzen C. 1988. The human central nervous system, 3rd ed. Berlin: Springer.

Nigg JT, Wong MM, Martel MM, Jester JM, Puttler LI, Glass JM, Zucker RA. 2006. Poor response inhibition as a predictor of problem drinking and illicit drug use in adolescents at risk for alcoholism and other substance use disorders. J Am Acad Child Adolesc Psychiatry. 454:468–475.

Nowicka A, Marchewka A, Jednoróg K, Tacikowski P, Brechmann A. 2011. Forgetting of emotional information is hard: an fMRI study of directed forgetting. Cereb Cortex. 213:539–549.

Ochsner KN, Bunge SA, Gross JJ, Gabrieli JDE. 2002. Rethinking feelings: an fMRI study of the cognitive regulation of emotion. J Cogn Neurosci. 14:1215–1299.

Ohman A. 2002. Automaticity and the amygdala: nonconscious responses to emotional faces. Curr Dir Psychol Sci. 112:62–66.

Page LA, Rubia K, Deeley Q, Daly E, Toal F, Mataix-Cols D, Murphy DG. 2009. A functional magnetic resonance imaging study of inhibitory control in obsessive-compulsive disorder. Psychiatry Res. 1743:202–209.

Phan KL, Fitzgerald DA, Nathan PJ, Moore GJ, Uhde TW, Tancer ME. 2005. Neural substrates for voluntary suppression of negative affect: a functional magnetic resonance imaging study. Biol Psychiatry. 573:210–219.

Preacher KJ, Hayes AF. 2004. SPSS and SAS procedures for estimating indirect effects in simple mediation models. Behav Res Methods Instrum Comput. 364:717–731.

Ruppin E, Schwartz EL, Yeshurun Y. 1993. Examining the volume efficiency of the cortical architecture in a multi-processor network model. Biol Cybernet. 701:89–94.

Sander D, Grandjean D, Pourtois G, Schwartz S, Seghier ML, Scherer KR, Vuilleumier P. 2005. Emotion and attention interactions in social cognition: brain regions involved in processing anger prosody. Neuroimage. 284:848–858.

Schmahmann JD, Pandya DN. 2006. Fiber pathways of the brain. Oxford: Oxford University Press.

Smith SM, Jenkinson M, Johansen-Berg H, Rueckert D, Nichols TE, Mackay CE, Behrens TE. 2006. Tract-based spatial statistics:

voxelwise analysis of multi-subject diffusion data. Neuroimage. 314:1487–1505.

Sokol-Hessner P, Camerer CF, Phelps EA. 2013. Emotion regulation reduces loss aversion and decreases amygdala responses to losses. Soc Cogn Affect Neurosci. 83:341–350.

Tibshirani R. 1996. Regression shrinkage and selection via the lasso. J R Stat Soc B. 267–288.

van den Wildenberg WP, van Boxtel GJ, van der Molen MW, Bosch DA, Speelman JD, Brunia CH. 2006. Stimulation of the subthalamic region facilitates the selection and inhibition of motor responses in Parkinson's disease. J Cogn Neurosci. 184:626–636.

Von Der Heide RJ, Skipper LM, Klobusicky E, Olson IR. 2013. Dissecting the uncinate fasciculus: disorders, controversies and a hypothesis. Brain. 1366:1692–1707.